

NEW OCCURRENCE OF FIRE OPAL FROM BEMIA, MADAGASCAR

Martina Simoni, Franca Caucia, Ilaria Adamo, and Pietro Galinetto

Twenty-two gem opals from a new volcanic deposit located near Bemia, in southeastern Madagascar, were investigated by classical gemological methods, SEM-EDS, powder X-ray diffraction analysis, LA-ICP-MS, and Raman and IR spectroscopy. Although none of the opals show play-of-color, they exhibit a wide variety of hues—including those typical of fire opal—that are related to iron content, mainly from Fe-rich inclusions. Consistent with their volcanic origin, these samples are microcrystalline and composed of opal-CT or opal-C. Among the inclusions are ilmenite needles, clay minerals, and iron oxides and hydroxides. The RI and, in particular, SG values are higher than those typical of natural fire opal (e.g., from Mexico) and some synthetic fire opal, allowing for a rapid separation.

Opals are water-bearing micro- and noncrystalline silica minerals, with the chemical formula $\text{SiO}_2 \cdot n\text{H}_2\text{O}$ (see, e.g., Graetsch et al., 1994; Downing, 2003; O'Donoghue, 2006). One attractive variety is fire opal, which is characterized by a red-orange-yellow bodycolor, with or without play-of-color (O'Donoghue, 2006). This opal variety does not have the typical structure of play-of-color opal; rather, it is composed of random aggregates of hydrated silica nanograins ~20 nm in diameter (Fritsch et al., 2006; Gaillou et al., 2008b).

The most famous locality for fire opal, one that has been producing fine material for more than 100 years, is the Querétaro area of Mexico (see, e.g., Koivula et al.,

1983; Gübelin, 1986). Other sources include the United States, Turkey, Australia, Indonesia, Ethiopia, Somalia, Kazakhstan, Canada, and Brazil (Ball and Daniel, 1976; Smith, 1988; Bittencourt Rosa, 1990; Holzhey, 1991; Bank et al., 1997; Enseli et al., 2001; O'Donoghue, 2006).

Opal, including the fire variety, is also known to come from various regions of Madagascar, particularly the Faratsiho deposit, located near the capital Antananarivo, in the center of the island (Lacroix, 1922). A new source of common opal, including fire opal (e.g., figure 1), was discovered a few years ago in the southeastern part of the island. According to A. and L. Pasqualini (pers. comm., 2010), who visited the deposit in May 2008, the opal is found near the city of Bemia, 70 km from the coast (figures 2 and 3). The opal occurs in Cretaceous rhyodacite volcanic rocks. Local people search for the opal by digging small pits, and ~200–400 kg of mixed-quality rough material has been produced. The opal generally occurs as nodules up to several centimeters in diameter or in veins up to 20–30 cm long, with large variations in quality and color. The rough opal is typically sent to the city of Antsirabe, 450 km north of Bemia, where it is fashioned into cabochons or faceted into fine gemstones that typically weigh up to 15 ct. Many of the various colors are typical of fire opal, but no play-of-color has been seen.

Building on the work of Simoni and Caucia (2009, in Italian), the present article describes the standard gemological properties of Bemia opal, as well as the inclusions, powder X-ray diffraction patterns, chemical composition, and spectroscopic features.

MATERIALS AND METHODS

We looked at 22 fashioned samples (0.32–21.05 ct, both faceted and cabochons) of opal from Bemia (e.g., figure 1), which were cut from material obtained by A. and L. Pasqualini at the mine. The specimens were examined by standard gemological methods to determine their optical properties, hydrostatic SG, UV fluorescence, and microscopic features.

Some inclusions in selected samples were characterized with a Zeiss Evo 40 scanning electron microscope

See end of article for About the Authors and Acknowledgments.
GEMS & GEMOLOGY, Vol. 46, No. 2, pp. 114–121.
© 2010 Gemological Institute of America

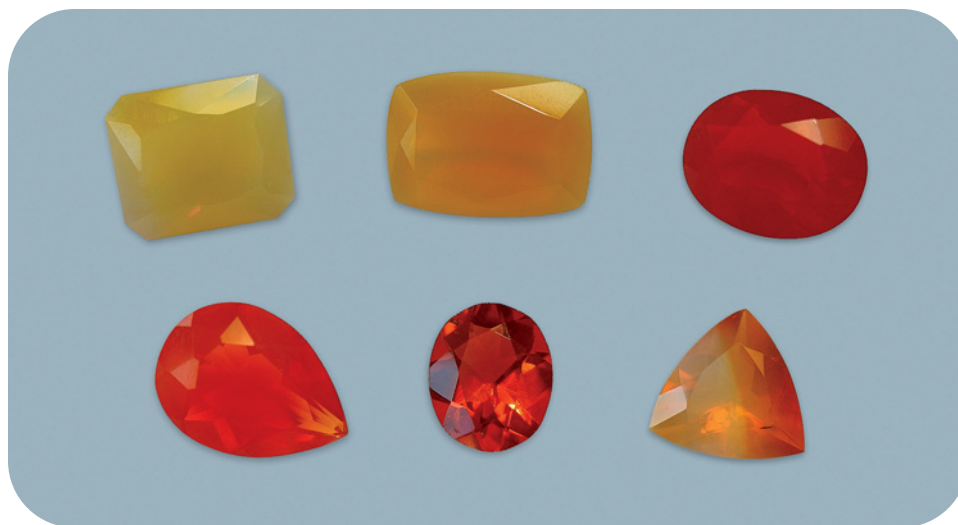


Figure 1. These fire opals (0.70–16.94 ct) are from a new deposit near Bemia, Madagascar. From left to right: top row—16.94 ct (sample no. 3), 3.96 ct (no. 5), 0.70 ct (no. 17); bottom row—1.40 ct (no. 21), 0.73 ct (no. 18), 2.88 ct (no. 14). Note the strong color zoning in sample 14. Composite photo by Andrea Pazzi.

(SEM) equipped with an Oxford Instruments energy-dispersive spectrometer (EDS), using an electron beam energy of 40 eV and a focal spot of 5 nm.

Laser ablation–inductively coupled plasma–mass spectrometry (LA-ICP-MS) was performed on four samples (nos. 3, 10, 18, and 22, selected to show a range of color). The instrument consisted of an Elan DRC-e mass spectrometer coupled with a Q-switched Nd:YAG laser source (Quantel Brilliant), with a fundamental emission (1064 nm) converted to 266 nm by two harmonic generators. The ablated material was transported to the mass spectrometer using helium as the carrier gas, mixed with Ar downstream of the ablation cell. The external and internal standards were NIST SRM 610 and Si, respectively. Four analyses per sample were collected, using a spot size of 50 μm . The results are reported in parts per million (ppm) by weight.

Powder X-ray diffraction (XRD) data were collected with a Philips PW 1800/10 diffractometer, using $\text{CuK}\alpha$ radiation in the range of 2° – 65° 2θ with a speed of 0.02° $2\theta/\text{sec}$. Since this is a destructive technique, we restricted these measurements to six samples (nos. 3, 10, 19, 20, 21, and 22) as designated by the Pasqualinis.

The Raman spectra of four samples (nos. 10, 20, 21, and 22) were recorded in the 3000 – 200 cm^{-1} range, using a Labram Dilor Raman H10 spectrometer equipped with an Olympus HS BX40 microscope and a cooled CCD camera as a photo-detector. The instrument employed an He-Ne laser (632.8 nm) as excitation radiation. A $100\times$ objective (numerical aperture = 0.99) was typically used, with a spatial resolution of $\sim 1\text{ }\mu\text{m}$ and depth resolution of $\sim 2\text{ }\mu\text{m}$.

We collected the mid-infrared (4000 – 400 cm^{-1}) spectra of three samples (nos. 3, 19, and 22) in transmission mode with a Nicolet Nexus FTIR spectrometer, using KBr pellets and operating with a resolution of 4 cm^{-1} .

RESULTS AND DISCUSSION

Gemological Properties and Inclusions. The appearance and gemological properties of the Malagasy opal samples are reported in table 1. They showed a wide range of colors

and transparency, sometimes with strong zoning (with a characteristic banded structure), but all had a resinous luster and no play-of-color (again, see figure 1). UV fluorescence varied greatly, in both color and intensity, from one sample to another and even within the same sample in some cases. Moreover, the stones with the most intense bodycolors had no UV reaction. No phosphorescence was observed in any specimens.

The RI values of 1.415–1.462 overlapped and extended

Figure 2. The volcanic deposit near Bemia, in south-eastern Madagascar, is a relatively new source of gem-quality opal.





Figure 3. At Bemia, opal is recovered from small pits by local residents. Photo taken in May 2008 by A. and L. Pasqualini.

below the typical range for opal in general (1.44–1.46; O'Donoghue, 2006), whereas they were slightly higher than those typical of other volcanic opals, such as the famous stones from Querétaro, Mexico (1.42–1.43, rarely down to 1.37; Koivula et al., 1983; Gübelin, 1986). The SG values we measured for the Bemia opal samples (2.05–2.38) were higher than those typically measured both for opal in general and for Mexican fire opal, which generally range from 1.98 to 2.20 for the former (O'Donoghue, 2006) and from 1.97 to 2.06 for the latter (Webster, 1994). Gaillou et al. (2004) attributed an unusually high SG value (2.18) in a white Madagascar opal to inclusions of cristobalite (a polymorph of SiO_2), which probably caused the milky appearance of their sample. Although this could well explain the high SG values in our samples, we did not find an obvious correlation between SG and the presence of a silica polymorph. The Malagasy opals also exhibited higher RI and SG values than the original Mexifire synthetic opals described by Choudhary and Bhandari (2008), which have an RI <1.40 and SG <1.77. However, they are similar to the values of the Mexifire synthetic manufactured since late 2009, which has an RI of 1.470 and an SG of 2.19 (G. Choudhary, pers. comm., 2010).

Crystalline inclusions were noted in some samples. Analysis by SEM-EDS identified dark opaque blebs as iron oxides (probably hematite; see, e.g., figure 4) and hydroxides; also present were needles of ilmenite. We determined that other inclusions were probably clay minerals, on the basis of their fibrous morphology and chemistry. Only seven samples had fluid inclusions (within small feathers) that were visible with the optical microscope.

With respect to the stability of the opal to dehydration and crazing, we did not observe any significant changes in

these samples during our observations over a period of ~1.5 years. However, we did not conduct any specific stability tests.

Chemical Composition. Trace-element chemistry is important for understanding some physical properties of gem opals, such as color and luminescence, and is a useful tool for determining their geologic and geographic origin (Gaillou et al., 2006, 2008a). The LA-ICP-MS data of four samples from Bemia are reported in table 2.

The four main impurities (>500 ppm) were: Mg

Figure 4. Opaque blebs, identified by SEM-EDS as hematite, are easily seen in this 11.03 ct opal, from which sample 19 was faceted. Photo by Andrea Pazzi.



TABLE 1. Gemological properties of 22 opal samples from Bemia, Madagascar.

Sample no.	Weight (ct)	Color	Diaphaneity	RI ^a	SG	UV fluorescence	
						Long-wave (366 nm)	Short-wave (254 nm)
1	9.30	Yellowish white	Translucent	1.460	2.19	Inert	Weak yellow
2	13.75	Yellow	Opaque	1.458	2.17	Inert	Weak green
3	16.94	Yellow and yellowish white	Translucent	1.458	2.15	Inert	Inert
4	21.05	Yellow	Translucent	1.449	2.15	Inert	Weak green
5	3.96	Yellowish orange	Translucent	1.439	2.11	Inert	Inert
6	0.38	Colorless	Transparent	1.419	2.19	Moderate yellow-green	Moderate yellow-green
7	0.39	Yellow	Translucent	1.415	2.19	Inert	Moderate blue (core) and moderate yellow-green (rim)
8	0.49	White	Translucent	1.416	2.35	Moderate blue	Moderate blue (core) and moderate yellow-green (rim)
9	0.55	White	Translucent	1.428	2.16	Moderate blue (core) and moderate yellow-green (rim)	Moderate blue (core) and moderate yellow-green (rim)
10	0.32	Yellowish white and yellow	Transparent	1.440	2.38	Moderate blue	Moderate blue
11	0.46	Yellow	Transparent	1.449	2.21	Moderate blue (core) and moderate yellow-green (rim)	Moderate blue (core) and moderate yellow-green (rim)
12	0.35	White	Translucent	nd	2.26	Weak blue	Moderate-weak yellow-green
13	0.49	White	Translucent	1.429	2.12	Weak blue (core) and weak yellow-green (rim)	Weak blue (core) and weak yellow-green (rim)
14	2.88	Orange and yellowish white	Translucent	1.439	2.15	Moderate blue	Moderate blue
15	11.56	Yellow	Transparent	1.450	2.15	Moderate blue (core) and moderate yellow-green (rim)	Moderate blue (core) and moderate yellow-green (rim)
16	2.94	Colorless	Transparent	1.462	2.18	Moderate blue (core) and moderate yellow-green (rim)	Moderate blue (core) and moderate yellow-green (rim)
17	0.70	Red	Translucent	1.460	2.20	Inert	Inert
18	0.73	Orange	Transparent	1.453	2.24	Inert	Inert
19	1.11	Yellow	Translucent	1.460	2.05	Inert	Inert
20	0.36	Orange	Translucent	nd	2.19	Inert	Inert
21	1.40	Orange	Translucent	1.460	2.15	Inert	Inert
22	0.86	Yellow	Translucent	nd	2.06	Inert	Weak yellow

^a Abbreviation: nd = not determined because too many fractures were present.

(~890–17,730 ppm); Al (~3000–5000 ppm, except for sample 3, with only 23 ppm); Ca (369–1314 ppm); and Cl (average 543 ppm). Aluminum, which substitutes for silicon, is typically the most common impurity in opal (Bartoli et al., 1990; Gaillou et al., 2008a). This substitution results in a charge balance that must be compensated by the mono- and divalent cations such as Na, Mg, K, and Ca, or the substitution of a hydroxyl ion for an oxygen to form silanol (Webb and Finlayson, 1987; Gaillou et al., 2008a). Aluminum can also occur as occlusions of clay particles (Webb and Finlayson, 1987), which is consistent with our SEM-EDS observations (see above). With respect to Ca, our Bemia samples were more enriched than the fire opals from Mexico, which may contain up to 490 ppm Ca (Gaillou et al., 2008a).

Sodium (~60–1200 ppm) was present in all the Bemia opals, as was Fe, which varied greatly (~140–12,070 ppm) according to color (again, see table 2). This is consistent

with the presence of Fe-containing inclusions (particularly Fe oxyhydroxides) causing the yellow and orange bodycolor (Rossman, 1994; Fritsch et al., 1999, 2002; Gaillou et al., 2008a); this, too, is in agreement with our SEM-EDS investigations. Other elements present in lesser amounts were, in order of decreasing average concentration: K, Zn, Ti, Ba, Zr, Sr, Be, Mn, Sc, Y, Cr, Ni, Rb, Pb, B, U, V, and Cu; Li and Co were always below 1 ppm. The Ba content of our samples (up to 42 ppm) is consistent with their volcanic origin (Gaillou et al., 2008a). With regard to chromophores other than Fe, all except Ti were less than ~10 ppm; Ti ranged from ~12 to 61 ppm (possibly due to the presence of ilmenite inclusions).

The green and blue luminescence of opal is known to be caused by uranium- or oxygen-related defects, respectively, though an excess of Fe³⁺ (>3000 ppm) may quench the effect (Fritsch et al., 1999; Gaillou et al., 2008a). Samples 3 and 18 were inert to both long- and short-wave

TABLE 2. Chemical composition (in ppm) of four opal samples from Bernia, Madagascar, as obtained by LA-ICP-MS.^a

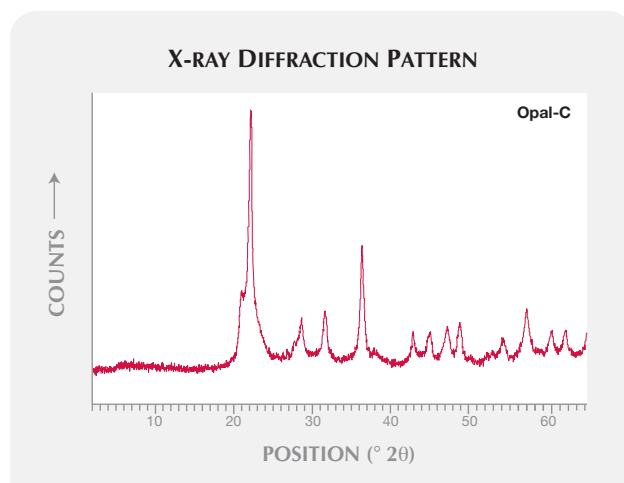
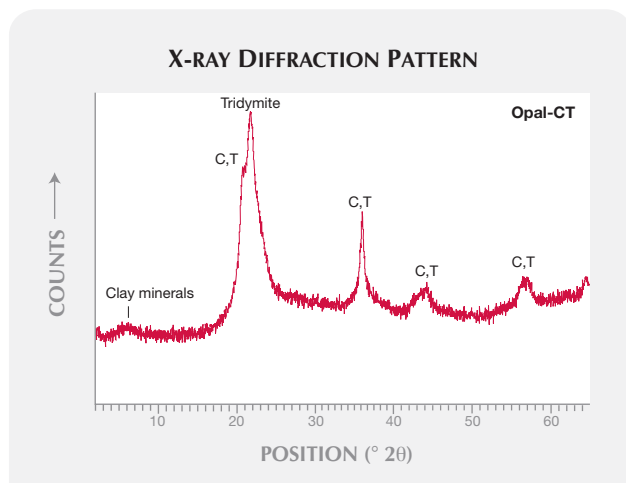
Element	No. 10 Yellowish white and yellow	No. 22 Yellow	No. 3 Yellow	No. 18 Orange
Li	0.15	0.21	0.30	0.44
Be	1.08	8.94	17.97	25.20
B	0.86	4.98	0.75	1.31
Na	1196	600.4	61.11	97.55
Mg	1122	891.0	5429	17730
Cl	412.3	453.1	443.7	870.4
Al	2890	3609	22.82	5040
K	336.2	197.2	51.73	398.9
Ca	1238	368.8	771.5	1314
Sc	3.09	4.60	3.09	2.70
Ti	53.76	61.29	15.15	12.10
V	0.30	3.30	0.29	1.66
Cr	1.02	3.77	1.40	5.90
Mn	1.09	12.44	10.97	9.73
Fe	137.1	1888	7251	12070
Co	0.41	0.73	0.18	0.39
Ni	0.78	4.44	2.24	2.98
Cu	0.20	1.70	0.53	1.61
Zn	1.09	6.98	71.09	86.56
Rb	3.89	1.38	0.36	3.44
Sr	43.40	10.69	1.68	2.28
Y	0.80	0.87	1.91	8.24
Zr	78.10	10.22	0.38	0.28
Ba	15.40	35.11	5.82	41.58
Pb	0.10	0.55	1.51	5.66
U	0.02	3.05	2.50	2.13

^a Average of four analyses per sample.

UV radiation (see table 1), which is consistent with their higher iron contents (>7000 ppm), despite the presence of U (>2 ppm). Sample 22, with 3 ppm U, was inert to long-wave UV but showed weak yellow fluorescence to short-wave UV, as would be expected from its Fe content (1888 ppm). Sample 10 exhibited blue (rather than green) luminescence, consistent with its low U and Fe contents; the oxygen-related defects causing this behavior cannot be measured by the techniques used on these samples.

X-ray Diffraction. Based on X-ray diffraction, according to Jones and Segnit's (1971) mineralogical classification, opal can be subdivided into three general groups: opal-C (relatively well ordered α -cristobalite), opal-CT (disordered α -cristobalite with α -tridymite-type stacking), and opal-A (amorphous). The powder X-ray diffraction measurements of four of the six samples analyzed by this method classified them as opal-CT, which is consistent with their volcanic origin (Jones and Segnit, 1971; Ostrooumov et al., 1999; Fritsch et al., 2004). Their patterns were characterized by main peaks in the 2θ range—attributed to cristobalite and tridymite phases—that showed various degrees of disorder (figure 5, left). The other two stones (nos. 20 and 21) can be considered opal-C on the basis of their X-ray patterns, which were similar to those of α -cristobalite (figure 5, right). Opal-C is also associated with volcanic deposits (Jones and Segnit, 1971), but in general it is rarer than opal-CT (Fritsch et al., 2004). Moreover, our results are consistent with the findings by Elzea and Rice (1996) that opal-C and opal-CT are part of a continuum of disor-

Figure 5. These powder X-ray diffraction patterns were collected from Malagasy samples consisting of opal-CT (left, no. 22) and opal-C (right, no. 21). The attribution of the main CT (cristobalite-tridymite) and tridymite peaks is shown for opal-CT, whereas all signals in the pattern on the right are related to cristobalite (the most important being the two peaks at 28.50° and 31.40° 2θ , which allow for a rapid identification). The broad band between 4.9° and 6.8° 2θ , especially visible in the pattern on the left, is due to clay minerals.



dered intergrowths between end-member cristobalite and tridymite stacking sequences.

The diffraction patterns of some samples also showed, in accordance with SEM-EDS observations, a broad band between 4.9 and $6.8^\circ 2\theta$, due to clay minerals. Identification of the specific clay mineral(s) requires further study.

Spectroscopy. Raman. This technique has been established as an effective, nondestructive method to characterize gem opal (Smallwood et al., 1997; Ostrooumov et al., 1999; Ilieva et al., 2007). The Raman spectra of our opal samples revealed several peaks between 3000 and 200 cm^{-1} , due to different stretching and bending vibration modes of the Si-O system (see, e.g., Smallwood et al., 1997). As expected, the most intense Raman peaks were located in the ~ 500 – 200 cm^{-1} range, which contains the typical features of tridymite and cristobalite (figure 6).

In the spectra of samples 10 and 22, we observed a broad band centered at $\sim 350\text{ cm}^{-1}$ and a weaker band at $\sim 300\text{ cm}^{-1}$, which are typical of opal-CT (e.g., Ostrooumov et al., 1999; Ilieva et al., 2007). These bands were not well resolved, as opal is a poor Raman scatterer, especially when a laser in the visible range (here, 632.8 nm) is used. Small features at 1086 , 955 , and 780 cm^{-1} were also present, together with a weak water signal at about 1620 cm^{-1} (not shown in figure 6).

Opal-C samples 20 and 21 exhibited Raman scattering at 412 and 226 cm^{-1} , revealing cristobalite as their dominant structural component (Ilieva et al., 2007), in agreement with the X-ray diffraction data. These peaks are broader than those of α -cristobalite, in accordance with the greater structural disorder of opal. However, they may contain contributions from inclusions of α -cristobalite, as suggested by Gaillou et al. (2004). The samples also contained minor peaks at 1620 , 1194 (in sample no. 21), 1090 , and 780 cm^{-1} .

Mid-Infrared. Although X-ray diffraction and Raman spectroscopy are the most informative techniques for determining an opal's structure and typology, IR spectroscopy can be usefully coupled with these other analytical methods. The IR spectra of the three opal-CT samples investigated (e.g., figure 7) were characterized by spectral features of molecular water and silanol (SiOH) groups, consisting of a broad absorption band at 3400 cm^{-1} and a feature at about 1650 – 1630 cm^{-1} (Farmer, 1974; Langer and Flörke, 1975; Bartoli et al., 1990). The three strong bands at ~ 1100 , 790 , and 470 cm^{-1} are related to the fundamental Si-O vibrations (see, e.g., Farmer, 1974; Plyusnina, 1979; Webb and Finlayson, 1987), whereas the two weak bands at ~ 2000 and 1880 cm^{-1} are probably due to overtones and combinations of Si-O fundamentals (Langer and Flörke, 1975). These IR spectra are consistent with the samples' microcrystalline nature, and in particular with their CT typology (see also Adamo et al., 2010).

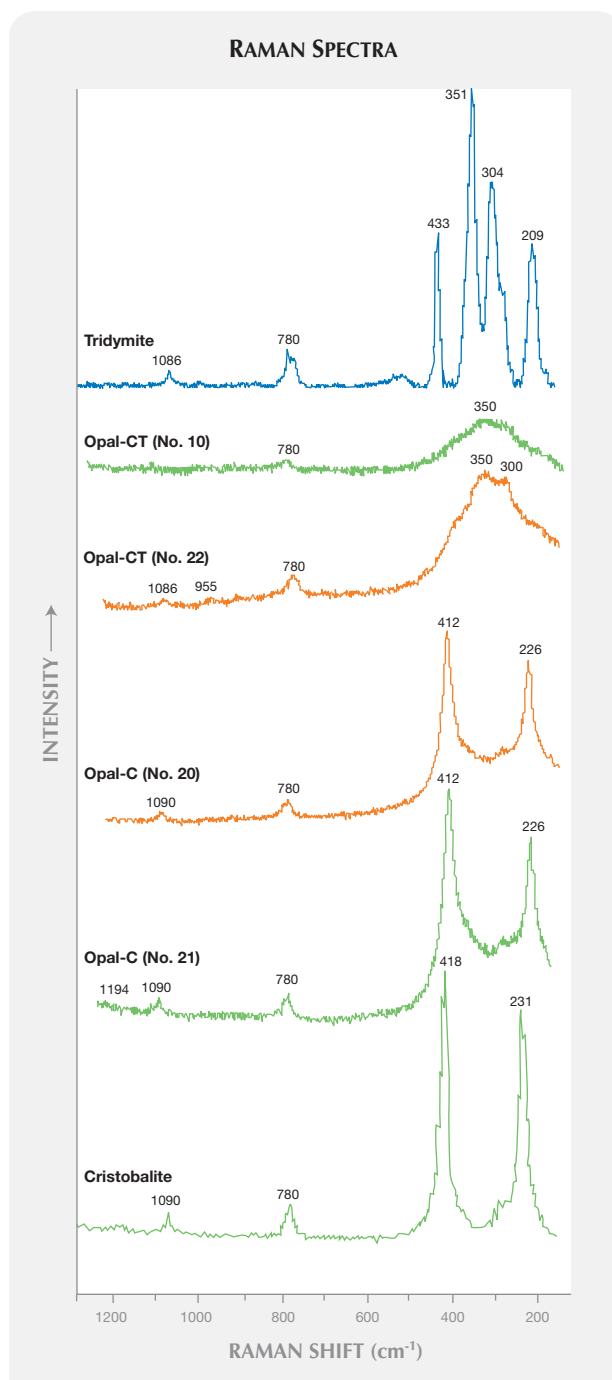


Figure 6. Raman spectra in the 1200 – 200 cm^{-1} range of the four Malagasy opals tested (nos. 10, 20, 21, and 22) are compared to those of standard α -cristobalite and α -tridymite minerals from the RRUFF database (rruff.info).

Clay-mineral impurities are responsible for the 3545 and 692 cm^{-1} absorption bands (Van Der Marel and Beitelspacher, 1976), which were observed in two of the three samples investigated.

MID-IR SPECTRUM

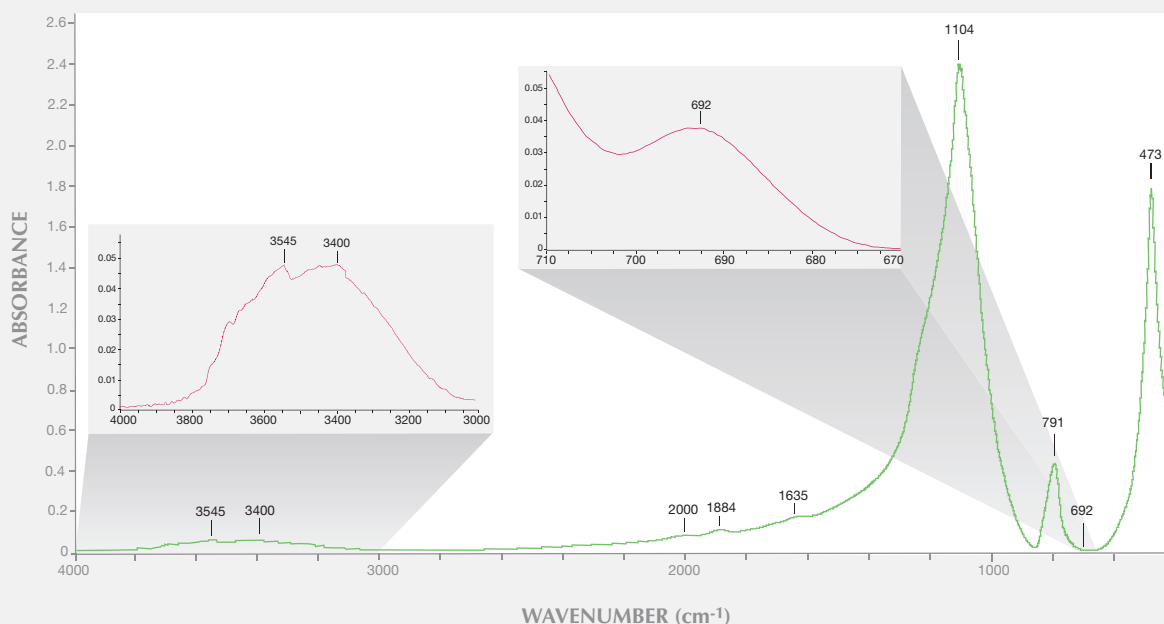


Figure 7. This mid-IR spectrum of an opal-CT sample (no. 22) shows features related to molecular water, SiOH groups, and Si-O bonds, as well as clay mineral impurities (insets).

IDENTIFICATION AND CONCLUSIONS

Opal samples from a new deposit near Bemia, Madagascar, show a wide variety of colors, including those typical of fire opal, but always without play-of-color and often with strong color zoning in a characteristic banded structure. Darker colors correspond to higher iron content (i.e., Fe-containing inclusions). The samples investigated here were all microcrystalline (opal-CT or opal-C) with varying degrees of order, as indicated by the X-ray diffraction data and Raman and IR spectra. The RI values (1.415–1.462) are higher than those typical of fire opals from other localities, such as Mexico, as are the SG values (up to 2.38), which

are also slightly higher than those reported for opal in general. The Malagasy opals are also distinguishable from the original Mexifire synthetics described by Choudhary and Bhandari (2008), on the basis of their higher RI and SG values. With respect to the Mexifire synthetic manufactured since late 2009, RI and SG are similar, though the slightly higher RI value of the new Mexifire material (1.470) should be diagnostic in most cases.

Opal from Bemia has been mined for a few years and is starting to enter the market. The material found so far, as well as ongoing work at the deposit, indicates the potential for economic production.

ABOUT THE AUTHORS

Dr. Simoni (arsimoni@tin.it) is a gemologist in Pavia, Italy. Dr. Caucia is professor of mineralogy in the Earth Sciences Department at the Università degli Studi di Pavia, Italy. Dr. Adamo is a postdoctoral fellow in the Earth Sciences Department at the Università degli Studi di Milano, and Dr. Galinetto is a researcher in the Theoretical Physics Department at the Università degli Studi di Pavia.

ACKNOWLEDGMENTS

The authors thank Armando and Luca Pasqualini of Pavia for providing samples and information about the opal investigated in this study. The authors are indebted to Giorgio Carbone and Marco Pelinzona (Università degli Studi di Pavia) for collaboration in X-ray diffraction data collection and SEM analyses, respectively, and to Dr. Alberto Zanetti (IGG-CNR, Pavia) for LA-ICP-MS measurements. Rajneesh Bhandari (Rhea Industries, Jaipur, India) and Gagan Choudhary (Gem Testing Laboratory, Jaipur) are acknowledged for information about the new Mexifire synthetic. The manuscript benefited considerably from thoughtful comments by Dr. Eloise Gaillou, Dr. Federico Pezzotta, and an anonymous reviewer.

REFERENCES

- Adamo I., Ghisoli C., Caucia F. (2010) A contribution to the study of FTIR spectra of opals. *Neues Jahrbuch für Mineralogie, Abhandlungen*, Vol. 187, No. 1, pp. 63–68.
- Ball R.A., Daniel A. (1976) Opal in south western Queensland: part one, a brief review; part two, some thoughts on Yowah Nuts. *Australian Gemmologist*, Vol. 12, No. 12, pp. 359–363.
- Bank H., Henn U., Milisenda C.C. (1997) Gems from Ethiopia. *Zeitschrift der Deutschen Gemmologischen Gesellschaft*, Vol. 46, No. 1, p. 4.
- Bartoli F., Bittencourt Rosa D., Doirisse M., Meyer R., Philippy R., Samama J.-C. (1990) Role of aluminium in the structure of Brazilian opals. *European Journal of Mineralogy*, Vol. 2, No. 5, pp. 611–619.
- Bittencourt Rosa D. (1990) Les opals nobles du district de Pedro II dans l'Etat de Piaui, region nord-est du Brésil. *Revue de Gemmologie A.F.G.*, Vol. 104, No. 1, pp. 3–7.
- Choudhary G., Bhandari R. (2008) A new type of synthetic fire opal: Mexifire. *G&G*, Vol. 44, No. 3, pp. 228–233.
- Downing P. (2003) *Opal Identification and Value*. Majestic Press, Estes Park, CO.
- Elzea J.M., Rice S.B. (1996) TEM and X-ray diffraction evidence for cristobalite and tridymite stacking sequences in opal. *Clay and Clay Minerals*, Vol. 44, No. 4, pp. 492–500.
- Ensels F., Kumbasar I., Eren R.E., Uz B. (2001) Characteristics of opals from Simav, Turkey. *Neues Jahrbuch für Mineralogie, Monatshefte*, Vol. 3, No. 5, pp. 97–113.
- Farmer V.C. (1974) *The Infrared Spectra of Minerals*. Mineralogical Society, London.
- Fritsch E., Rondeau B., Ostrooumov M., Lasnier B., Marie A.-M., Barrault A., Wery J., Connoué J., Lefrant S. (1999) Découvertes récentes sur l'opale. *Revue de Gemmologie*, No. 138/139, pp. 34–40.
- Fritsch E., Ostrooumov M., Rondeau B., Barreau A., Albertini D., Marie A.-M., Lasnier B., Wery J. (2002) Mexican gem opal: Nano and micro-structures, origin of color and comparison with other common opals of gemmological significance. *Australian Gemmologist*, Vol. 21, No. 6, pp. 230–233.
- Fritsch E., Gaillou E., Ostrooumov M., Rondeau B., Devouard B., Barreau A. (2004) Relationship between nanostructure and optical absorption in fibrous pink opals from Mexico and Peru. *European Journal of Mineralogy*, Vol. 16, No. 5, pp. 743–752.
- Fritsch E., Gaillou E., Rondeau B., Barreau A., Albertini D., Ostrooumov M. (2006) The nanostructure of fire opal. *Journal of Non-Crystalline Solids*, Vol. 352, pp. 3957–3960.
- Gaillou E., Mocquet B., Fritsch E. (2004) Gem News International—A new gem material from Madagascar: A mixture of cristobalite and opal. *G&G*, Vol. 40, No. 4, pp. 339–340.
- Gaillou E., Delaunay A., Fritsch E., Bouhnik-le-Coz M. (2006) Geologic origin of opals deduced from geochemistry. *G&G*, Vol. 42, No. 3, p. 107.
- Gaillou E., Delaunay A., Rondeau B., Bouhnik-le-Coz M., Fritsch E., Corner G., Monnier C. (2008) The geochemistry of gem opals as evidence of their origin. *Ore Geology Reviews*, Vol. 34, pp. 113–126.
- Gaillou E., Fritsch E., Aguilar-Reyes B., Rondeau B., Post J., Barreau A., Ostrooumov M. (2008) Common gem opal: An investigation of micro- to nano-structure. *American Mineralogist*, Vol. 93, pp. 1865–1873.
- Graetsch H., Gies H., Topalovi I. (1994) NMR, XRD and IR study on microcrystalline opals. *Physics and Chemistry of Minerals*, Vol. 21, No. 3, pp. 166–175.
- Gübelin E.J. (1986) Opal from Mexico. *Australian Gemmologist*, Vol. 16, No. 2, pp. 45–51.
- Holzhey G. (1991) Feueropal aus Aleksejewskoje, Kasachische, UdSSR – ein Beitrag zu vergleichenden gemmologisch-mineralogische Untersuchungen mikrokristalline SiO₂-Minerale. *Zeitschrift der Deutschen Gemmologischen Gesellschaft*, Vol. 40, No. 1, pp. 11–13.
- Ilieva A., Mihailova B., Tsintov Z., Petrov O. (2007) Structural state of microcrystalline opals: A Raman spectroscopic study. *American Mineralogist*, Vol. 92, pp. 1325–1333.
- Jones J.B., Segnit E.R. (1971) The nature of opal. I. Nomenclature and constituent phases. *Journal of the Geological Society of Australia*, Vol. 18, No. 1, pp. 57–68.
- Koivula J.L., Fryer C., Keller P.C. (1983) Opal from Querétaro, Mexico: Occurrence and inclusions. *G&G*, Vol. 19, No. 2, pp. 87–96.
- Lacroix A. (1922) *Minéralogie de Madagascar*, Vol. 1. Augustin Challamel éditeur, Paris, pp. 269–273.
- Langer K., Flörke O.W. (1975) Near infrared absorption spectra (4000–9000 cm⁻¹) of opals and the role of “water” in these SiO₂ · nH₂O minerals. *Fortschritte der Mineralogie*, Vol. 52, No. 1, pp. 17–51.
- O'Donoghue M., Ed. (2006) *Gems*, 6th ed. Butterworth-Heinemann, Oxford, UK.
- Ostrooumov M., Fritsch E., Lasnier B., Lefrant S. (1999) Spectres Raman des opales: Aspect diagnostique et aide à la classification. *European Journal of Mineralogy*, Vol. 11, No. 5, pp. 899–908.
- Plusnina I.I. (1979) Infrared spectra of opals. *Soviet Physics Doklady*, Vol. 24, No. 5, pp. 332–333.
- Rossmann G.R. (1994) Colored varieties of the silica minerals. In P.J. Heaney, C.T. Prewitt, G.V. Gibbs, Eds., *Silica—Physical Behavior, Geochemistry and Materials Applications*, Reviews in Mineralogy and Geochemistry, Vol. 29, Mineralogical Society of America, Washington, DC, pp. 433–467.
- Simoni M., Caucia F. (2009) Opali di fuoco dal Madagascar. *Rivista Gemmologica Italiana*, Vol. 4, No. 2, pp. 91–104.
- Smallwood A.G., Thomas P.S., Ray A.S. (1997) Characterisation of sedimentary opals by Fourier transform Raman spectroscopy. *Spectrochimica Acta*, Part A, Vol. 53, pp. 2341–2345.
- Smith K.L. (1988) Opals from Opal Butte, Oregon. *G&G*, Vol. 24, No. 4, pp. 229–236.
- Van Der Marel H.W., Beutelspacher H. (1976) *Atlas of Infrared Spectroscopy of Clay Minerals and Their Admixture*. Elsevier, Amsterdam.
- Webb J.A., Finlayson B.L. (1987) Incorporation of Al, Mg, and water in opal-A: Evidence for speleothems. *American Mineralogist*, Vol. 72, pp. 1204–1210.
- Webster R. (1994) *Gems: Their Sources, Descriptions and Identification*, 5th ed. Rev. by P.G. Read, Butterworth-Heinemann, Oxford, UK.

For online access to all articles in **GEMS & GEMOLOGY** from 1981 to the present, visit:

gia.metapress.com